



INFLUENCE OF CABLE TENSION ON THE DYNAMIC STABILITY OF A LARGE MULTI-SPAN CABLE-STAYED BRIDGE

Nijat MASTANZADE^{1,a*}, Tural RUSTAMLI^{2,b}, Nariman ABDINLI^{3,c}

¹Azerbaijan Technical University, Baku, Azerbaijan

²Hydrotrans Engineering Ltd., Baku Azerbaijan

³Sumgayit Technology Park, Sumgayit, Azerbaijan

E-mail: ^{a*}nijat.mastan@gmail.com, ^brustamli.tural.90@gmail.com, ^cn.abdinli@outlook.com

<https://doi.org/10.61413/RUUM1114>

Abstract: Large-span cable-stayed bridges are increasingly becoming a vital component of modern bridge infrastructure due to their efficiency in load distribution, aesthetic appeal, and ability to span significant distances. This study examines the structural and dynamic performance of Azerbaijan's largest multi-span cable-stayed bridge, which is currently under construction along the Muganly-Ismayilli-Gabala road. With a total length of 1100 meters, the bridge is located in a region of high seismic activity, making stability and structural integrity paramount concerns in its design and construction. A detailed load analysis was conducted, considering both permanent and temporary loads. These include the self-weight of the bridge, vehicle loads, environmental forces such as wind, snow, and ice, as well as the influence of seismic effects. The bridge features multiple cable configurations - 31×6", 37×6" and 48×6"—each with specific cross-sectional areas and tension forces that ensure structural stability. To mitigate seismic impact, the bridge is equipped with kinematic roller supports between the stiffening beam and its supporting structures, allowing controlled movement during seismic events. The study also focuses on the dynamic behavior of the bridge under various forces, particularly wind loads that induce oscillations in the cables and the stiffening beam. Through finite element analysis, the vertical and horizontal vibration frequencies were calculated, ensuring that resonance conditions are avoided. The results demonstrate that the bridge remains within safe limits for aerodynamic stability, with no risk of excessive oscillations due to wind or traffic loads. Furthermore, the analysis of cable strength and durability confirms that the maximum tension forces are within acceptable limits, with safety margins that comply with international engineering standards. The bridge's stiffness conditions were verified using deformation calculations, showing that maximum deflections remain within allowable limits, ensuring long-term serviceability. This study provides crucial insights into the design and performance of large-span cable-stayed bridges in seismically active regions. The findings highlight the importance of advanced structural analysis and innovative engineering solutions to enhance stability, durability, and safety. The research contributes to the broader understanding of bridge engineering, offering valuable guidelines for the construction of future large-span cable-stayed structures in challenging environmental conditions.

Keywords: *cable-stayed, bridge, strength, dynamic stability, durability*

Introduction.

Large-span cable-stayed bridges are increasingly dominating the bridge infrastructure. These structures consist of one or more pylons connected to the roadbed by means of steel ropes—cables [1-5]. The pylons, in turn, are not connected to the bridge supports. For example, this work examines

the project of the largest multi-span cable-stayed bridge in Azerbaijan, currently under construction on the Muganly-Ismayilli-Gabala road [6]. This bridge has a total length of 1000m (Fig. 1). Considering that the construction site of the bridge is located in a region of high seismic activity, the issue of dynamic stability is highly relevant. To reduce the response to seismic shocks, kinematic roller supports are provided between the bridge's stiffening beam and the supports. The A–15 live load has been selected, representing a vehicle load with an axial force of 15kN , applied to the bridge in accordance with regulatory guidelines.



Fig 1. General view of the bridge

Forces on the bridge cables. In addition to its own weight, the cables of the cable stayed bridge are influenced by the weight of the transition shooting range, the weight of snow and ice that has fallen on the cable, the wind load, and the pre-tension force of the cable (Fig. 2). Loads entering the bridge are collected from permanent (weight of the bridge beam and road surface on it, railings and paving) and temporary (load falling from automobile tires) loads. Moreover, the bridge in this example is situated in a highly seismic zone [5]. Constant load per running meter is $P = P_1 + P_2 = 83,7 + 105 = 188,7 \text{ kN/m}$. The live load per running meter is taken as $q = 128 \text{ kN/m}$. Detailed information about implemented loads is given in Table 1.

Table 1. Loads caused by bridge loads

Load class	Calculation data				Reliability coefficient	Loads	
	width (m)	height (m)	area (m ²)	Volume weight (kg/m ³)		Normative g_n (kN)	Design g_h (kN)
Waterproofing	24.6	0.01	0.246	1.60	1.30	0.39	0.512
Asphalt concrete roadway	18.00	0.07	1.260	2.30	1.50	2.90	4.347
Sidewalk	0.75	0.06	0.045	2.50	1.10	0.11	0.12
Border	0.50	0.90	-	-	1.10	1.50	1.694
Border	0.50	0.90	-	-	1.10	1.50	1.694
Only 1 linear meter						6.48	8.370

Dead load of the beam was taken into account when calculating according to the CSI Bridge V21.2.0 program.

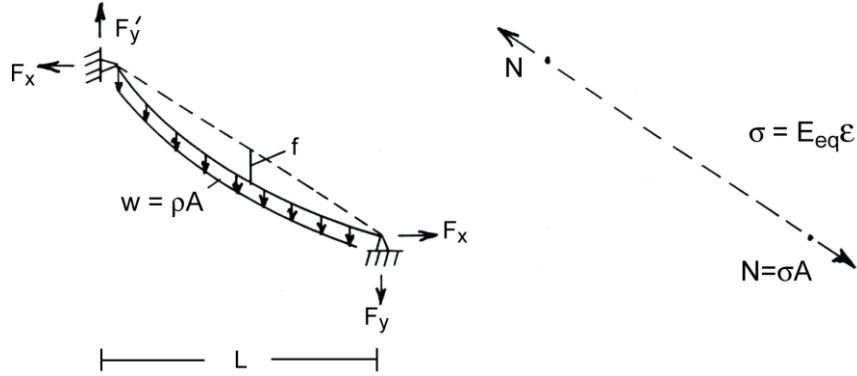


Fig.2. Appearance of external and internal forces falling on the cable rope: horizontal and vertical projections of the tension force F_x and F_y cable; f is cable inclination; w is a load on the lead; E_{eq} is equivalent modulus of elasticity; N is a tension force

Three transverse cables were used on the bridge: $31 \times 6''$, $37 \times 6''$ and $48 \times 6''$. Their cross-sectional areas are as follows: $A_1 = 56,55 \text{ cm}^2$, $A_2 = 67,488 \text{ cm}^2$ and $A_3 = 87,36 \text{ cm}^2$. For one span $L = 200 \text{ m}$ $31 \times 6''$ 14 units of cross section, $37 \times 6''$ 20 units of cross section and $48 \times 6''$ 2 units of cross section. The cable-stayed bridge features a harp-shaped design (Fig. 3).

Cable hardness is calculated based on elastic stiffness K_E and geometric stiffness K_g . The reduction in load on the cables caused by each stress results in their inclination, which subsequently induces vibrations in the structure by formula (1) [7].

$$K_I = K_E + K_g = \frac{EA_i}{l_0} \begin{bmatrix} \cos^2 \theta & \cos \theta \sin \theta \\ \cos \theta \sin \theta & \sin^2 \theta \end{bmatrix} + \frac{N}{L} \begin{bmatrix} 1 & 0 \\ 0 & 1 \end{bmatrix} \quad (1)$$

Where E is the modulus of elasticity of the cable material; A_i is the cross sectional area of the i -cable element; l_0 is a length of unstressed cable; $\cos \theta$, $\sin \theta$ are angular function of cable stiffness to the horizontal region; N is the longitudinal tension;

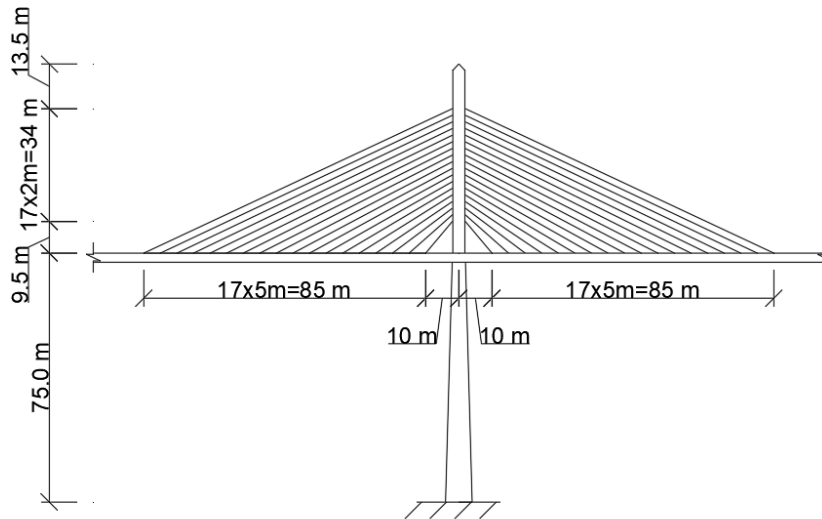


Fig. 3. View of cables falling on the right and left side of the bridge pylon

Nijat MASTANZADE, Tural RUSTAMLI, Nariman ABDINLI
Influence of cable tension on the dynamic stability of a large multi-span cable-stayed bridge

The tension of the cables is calculated separately and shown in Table 2. Here, for cables of type $31 \times 6''$ total $\sum N_1 = 2(1294 + 1305,1 + 1407,3 + 1403,7 + 1611,7 + 1726,7 + 1825,7) = 21148,4kN$;

For cables of type

$37 \times 6''$ $\sum N_1 = 2(2141 + 2176,7 + 2293 + 2410,6 + 2523,4 + 2633,7 + 2776,6 + 2971,4 + 3180,2 + 3244,7) = 52702,6kN$

For cables of type $48 \times 6''$ $\sum N_3 = 2(3907,4) = 7814,8kN$

And the resulting stress will be by formula (2) [8,9]:

$$\sigma = \frac{\sum N}{A_k} = \frac{(21148,4 + 52703,2 + 7814,8)10^3 N}{5655 \times 14 + 6748 \times 20 + 8736 \times 2} = 352,6MPa \quad (2)$$

Table 2. Tension forces and cross section of cables on one side of the bridge

TABLE: Element Forces - Frames			
Frame	OutputCase	P	Cable section
Text	Text	Tonf	
13709	ENV-NL(ULS)-	129.40	31x0.6"
13708	ENV-NL(ULS)-	130.51	31x0.6"
13707	ENV-NL(ULS)-	140.73	31x0.6"
13706	ENV-NL(ULS)-	140.37	31x0.6"
13705	ENV-NL(ULS)-	161.17	31x0.6"
13704	ENV-NL(ULS)-	172.67	31x0.6"
13703	ENV-NL(ULS)-	182.57	31x0.6"
13702	ENV-NL(ULS)-	214.10	37x0.6"
13701	ENV-NL(ULS)-	217.67	37x0.6"
13700	ENV-NL(ULS)-	229.30	37x0.6"
13699	ENV-NL(ULS)-	241.06	37x0.6"
13698	ENV-NL(ULS)-	252.34	37x0.6"
13697	ENV-NL(ULS)-	263.37	37x0.6"
13696	ENV-NL(ULS)-	277.66	37x0.6"
13695	ENV-NL(ULS)-	297.14	37x0.6"
13694	ENV-NL(ULS)-	318.02	37x0.6"
13693	ENV-NL(ULS)-	324.47	37x0.6"
13692	ENV-NL(ULS)-	390.74	48x0.6"

The maximum cable tension force was taken as $\sum P_{un} = 8700kN$. Then, you can calculate the resistance of the cable as follows by formula (3) [12,13]:

$$R_{dh} = k \frac{\sum P_{un}}{A \gamma_m} = 0,87 \times \frac{8700 \times 10^3}{2755 \times 1,6} = 1717,1MPa \quad (3)$$

where $k = 0,87$ is a coefficient of the strength coefficient; $\gamma_m = 1,6$ reliability factor. Cable strength condition is:

$$\frac{N_{max}}{A_k} = \frac{3907,4}{8736} = 447MPa < R_{dh} \times m \times m_1 = 1717,1 \times 1 \times 0,8 = 1416,88MPa \quad (4)$$

The strength condition of cable cables is satisfied. Here are the working condition coefficients m and m_1 .

The cable durability condition is checked using the following formula:

$$\sigma_{max} = 352,6MPa \leq m_1 \gamma_w R_{dh} m = 0,83 \times 0,9 \times 1717,1 \times 1 = 1282,67MPa \quad (5)$$

The cable rope continuity condition is satisfied. Here, γ_w is a factor that accounts for the change

in stress.

Stiffness condition of Cable-stayed bridge beam

The stiffness condition for large bridges is checked using the following formula (6) [2,3]:

$$\frac{y_{\max}}{L} \leq \frac{L}{400} \quad (6)$$

The maximum deflection from the design one span on the middle of the bridge and is $y_{\max} = 482\text{mm}$. Then on the left side of the formula $0,00241 < 0,0025$. The condition is satisfied.

Dynamic model and analysis of structure. The wind load acting on the structure primarily moves the cables, causing the stiffening beam to oscillate. The cables and the stiffening beam begin to sway due to aerodynamic forces, with movements being mainly vertical and horizontal. The most dangerous of these is the vertical oscillation of the stiffening beam. The differential equation can be written as follows by formula (7) [8,9,11]:

$$M\ddot{u} + C\dot{u} + Ku = -F_{\text{eff}} \quad (7)$$

Here, M is the mass of the dynamic system; C is damping characteristic; K is a stiffness of the system; \ddot{u} , \dot{u} , u are displacement, speed and acceleration respectively; F_{eff} is a dynamic force acting on it. When solving the problem by the finite element method, we can write the equation of free oscillations as follow

$$[M_i][\ddot{u}_i] + [C][\dot{u}_i] + [K][u] = 0 \quad (8)$$

Here $[M]$, $[C]$, $[K]$, $[u]$ are the mass, damping, stiffness and displacement matrices, accordingly.

The first and second frequency of vertical vibration can be determined from below formula (9) [3]:

$$\omega_{v,i} = \sqrt{A_i \times \frac{g}{H_i} \times \frac{E_v}{R_v} \times \frac{(p+v)}{p} \times \frac{n}{\left[1 + \frac{(n-1)^2 l^2}{4n^2 H_p^2}\right]}} \quad (9)$$

Here A_i is the coefficient for the i oscillation mode, $A_1 = 0,35$; g - free fall acceleration; H_p - the height of the pylon, $H_p = 57\text{m}$; E - modulus of elasticity of the cable, $E = 1,6 \times 10^5 \text{ mPa}$; p - constant load on the crossing beam, $p = 188,7 \text{ kN/m}$; v is a temporary load on the crossing beam, $v = 128 \text{ kN/m}$; n is the number of panels in one deck, $n = 36$; l is a maximum span, $l = 200\text{m}$.

For the first mode ($i = 1$, $A_1 = 0,35$), the frequency of vertical oscillation is

$\omega_{v_1} = 20,20 \text{ rad/sec}$. Then the period will be:

$$T_{v_1} = \frac{2\pi}{\omega_{v_1}} = 0,31 \quad (10)$$

For the second mode ($i = 2$, $A_2 = 0,35$) the frequency of vertical oscillation is

$\omega_{v_2} = 30,08 \text{ rad/sec}$.

$$T_{v_2} = \frac{2\pi}{\omega_{v_2}} = 0,208 \text{ sec} \quad (11)$$

Nijat MASTANZADE, Tural RUSTAMLI, Nariman ABDINLI
Influence of cable tension on the dynamic stability of a large multi-span cable-stayed bridge

The resonance period for automobile bridges and cable stayed pedestrian crossings is $T_v = (0,45 \div 0,6 \text{Ssec})$. In the first and second mode of vertical oscillations, the period remains outside the resonance range.

The frequency of horizontal oscillations for the third mode ($i = 1, 2, 3$) is calculated by formula (12) [3]:

$$\omega_{h,i} = \sqrt{\frac{i^4 \pi E I_h}{l^4 n} + \frac{g}{H_p}} \quad (12)$$

Here I_h is the moment of inertia in the horizontal direction of the stiffness beam, $I_h = 550 \text{m}^4$; $E = 2,06 \times 10^7 \text{mPa}$; $m = p/g = 83,7/9,81 = 8,53 \text{kN/m}$ mass of 1 long meter of the beam.

For the first mode ($i = 1$), the frequency of oscillations in the horizontal direction is $\omega_{h,1} = 5,12 \text{rad/sec}$ and the period:

$$T_{v1} = \frac{2\pi}{\omega_{v1}} = 1,226 \text{sec} \quad (13)$$

For the second mode ($i = 2$), the frequency of oscillations in the horizontal direction is $\omega_{h,2} = 10,22 \text{rad/sec}$ and the period:

$$T_{v2} = \frac{2\pi}{\omega_{v2}} = 0,61 \text{sec} \quad (14)$$

For the third mode ($i = 3$), the frequency of oscillations in the horizontal direction is $\omega_{h,3} = 15,32 \text{rad/sec}$ and the period:

$$T_{v3} = \frac{2\pi}{\omega_{v3}} = 0,41 \text{sec} \quad (15)$$

Period values of horizontal oscillations are outside the range of critical value $T_h = (0,9 \div 1,2 \text{sec})$. The period of both oscillations' mode does not reach the critical value for all modes. The main condition of the study is the generation of aerodynamic waves during the critical wind speed:

$$V_{cr} > 1,5V_p \quad (16)$$

Here $V_p = 32 \text{m/sec}$ maximum wind speed in the construction site. The critical speed is determined by the following formula (17):

$$V_{cr} = V_{cr,m} \times \omega_t \times B \quad (17)$$

Here $B = 24,6 \text{m}$ - the maximum width of the pedestrian crossing; V_{cr} , $m = 8,0 \text{m/sec}$ critical speed determined on the model. Frequency of rotational oscillations $\omega_t = 2,5\omega_{v1} = 2,5 \times 20,20 = 50,5 \text{rad/sec}$. The frequency of the first mode of vertical oscillations is $\omega_{v1} = 20,20 \text{rad/sec}$.

$$V_{cr} = 8,0 \times 50,5 \times 24,6 = 9938,4 \text{rad/s} > 1,5 \times 45 = 67,5 \text{m/sec} \quad (18)$$

The aerodynamic stability condition is within limit.

Conclusion. 1) the load pattern considered includes the bridge's self-weight and a live load modeled as A-15, representing a four-axle vehicle load; 2) the tension force of the cables plays a critical role in the dynamic stability of cable-stayed bridges. Therefore, it is essential to evaluate the strength and durability of the cables as well as the stiffness conditions of the bridge beams. The

Ismailli Bridge project, serving as a reference, adheres to these requirements; 3) damage or removal of components from the structural system alters the stress-strain state of the bridge. For instance, wire breakage within the anchorage reduces the tension in the cables, leading to a decrease in pulling force, cable oscillation, and an increase in the deflection of the stiffening girder; 4) to ensure proper maintenance and operation of the bridge, it is crucial to assess the stress levels in the cables, either in situ or under laboratory conditions.

REFERENCES

- [1]. AzDTN 2.1-1. *Loads and influence*. Baku.2015
- [2]. AzDTN 2.05.03.84. *Bridge and pipes*. Bakı.2011
- [3]. AASHTO LRFD. *Bridge Design Specification*. 8th Ed.Sept.2017
- [4]. F. Yang, H. Zhao, A.L, Z. Fang. *Experimental-numerical analysis on the cable vibration behavior of a long-span rail-cum-road cable-stayed bridge under the action of high-speed trains*, Applied Science.2023,13,11082
- [5]. Papadopolus P.G., J. Arethas, P. Lazaridis. *Numerical study on the behavior of cables of cable-stayed bridges. Earthquake Resistant Engineering*. WIT Transaction on the Built Environment, Vol.81. 2005
- [6]. Muganli-Ismailli-Gabala road reorganization. *Bridge over Aksu river. Design Project*. Euroscon. Baku.2020
- [7]. B.M. Al-Washali, Z. Yifeng, G. Xin, C. Xiaoxu, A. Al-Washali. *Structural Dynamic Analysis of cable-stayed bridge due to cable failure under unexpected events*. Int. Journal of Scientific & Technology Research. Vol. 10, Issue 03, March 2021
- [8]. Y. Zeng, Y. Zeng, H. Yu, Y. Tan, H. Tan, H.Zheg. *Dynamic characteristics of a double pylon cable-stayed bridge with steel trucs girder and single-cable plane*. Advanced in Civil Engineering. V. 2021.
- [9]. X. Zhu, Y. Jiang, G. Weng. *Study of the dynamic reaction mechanism of the cable-stayed tube bridge under earthquake action*. Buildings 2024, 14, 2009
- [10]. D. Huang, W. Chen. *Cable structures in bridge engineering*. J. Bridge engineering, 2019, 24(8), 02019001
- [11]. M. Husem, S. Pul, Y. Zandi, M.E. Arslan. *The behavior of cable-stayed bridge having different cable arrangements under static and dynamic loads*. Recent researches in geography, Geology, energy. Environment and biomedicine
- [12]. H. Dehghani, E. Deghani, M. Sharifi, S.R. Hoseini Vaer. *Effect of initial cable tension on cable-stayed bridge performance and a new construction method*. J. of rehabilitation in civil engineering 12-4 (2024) 136-154
- [13]. P. Jakiel, Z. Maniko. *Estimation of cables tension of cable-stayed footbridge using measured natural frequencies*. MATEC Web of confrence

Received: 13.01.2025

Accepted: 04.05.2025